Northwestern Medicine®
Feinberg School of Medicine

Integrating Bioinformatics with Transplant Research at Comprehensive Transplant Centre

Bioinformatics at CTC

Bioinformatics core as a research support, primarily for CTC members

Provides state-of-the-art bioinformatics training and analytic support services to investigators interested in basic, pre-clinical, clinical and epidemiological transplant studies, within and outside Northwestern University

Works as a platform such that CTC and other NU researchers could do collaborative research works involving data from -

- Genomics and Transcriptomics studies
- Proteomics and Metabolomics - experiments
- Public Databases

Bioinformatics Core at CTC

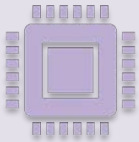

Bioinformatics core is focused to analyze high throughput and/or high-dimensional biological data arising from diverse technology platforms, including but not limited to,

Arrays: Gene expression, transcript/isoform, SNP, Exon, methylation

Next Generation Sequencing: DNA-seq, RNA-seq, WES, ChIP-seq, etc.

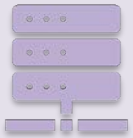

Core utilizes NU's High Performance Computing Cluster, QUEST

Supports data storage

(Currently up to 5 Tb)

QUEST6

- Number of Nodes: 184 nodes and 5152 cores total, 28 cores/node
- Processor: Intel Xeon E5-2680, v4 14C 2.4 GHz
- Memory: Per node (Per Core) 128 GB
- Type: DDR4 1866 MHz
- Number of GPU nodes: 15

- Core provides various analysis services, including but not limited to,
  - Sequencing data processing, Differential gene/isoform analysis, Gene Set Enrichment Analysis, Pathway Analyses, Class discovery, pattern recognition, Genome Wide Association Studies, and Transcription factor binding site analysis
    - Micro-array
    - RNA-Seq
    - ImmunoSeq
    - ChIP-Seq
    - Single-cell Seq
    - Metabolomics
    - Proteomics

Micro-Arrays

- feature extraction

- quality control

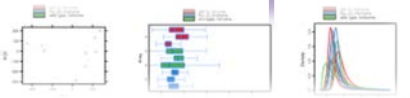

- Normalization / batch effect correction
- Differential expression analysis / feature Selection

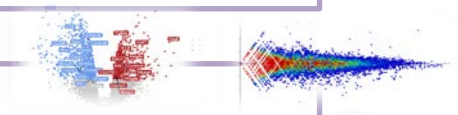

- Clustering/Classification

- biological interpretation of the results

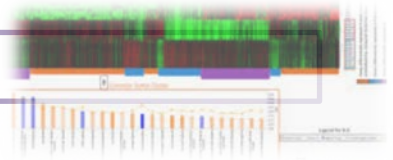

Kidney Transplant + arrays + machine learning

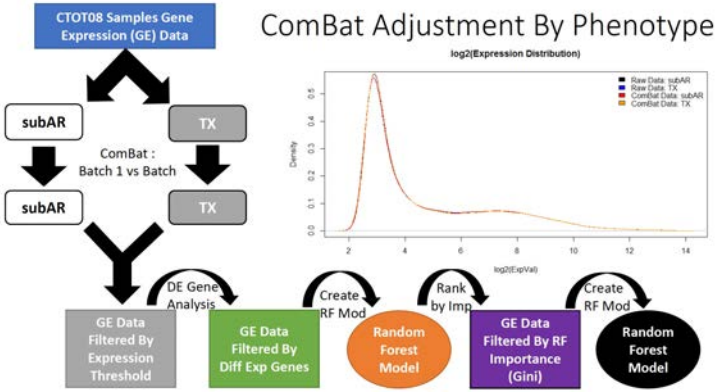

Data Set	Paied Samples, n	TX: subAR (% subAR prevalence)	Probability Threshold	% Negative (spared biopsy)	NPV	True Negative	False Negative	% Positive (pickup subAR)	PPV	True Positive	False Positive
Discovery Set	530	400:130 (24.5)	0.375	74.7	88	349	42	25.3	61	83	51
Validation set 1	138	96:42(30.4)	0.375	71.7	78	77	22	28.3	51	20	19
Validation set 2	129/138	93:36(27.9)	0.375	72.1	80	74	19	27.9	47	17	19

Friedewald et al, Development and clinical validity of a novel blood-based molecular biomarker for subclinical acute rejection following kidney transplant, Am J Transplant . 2019 Jan;19(1):98-109

Kidney Transplant + arrays + machine learning

IPA

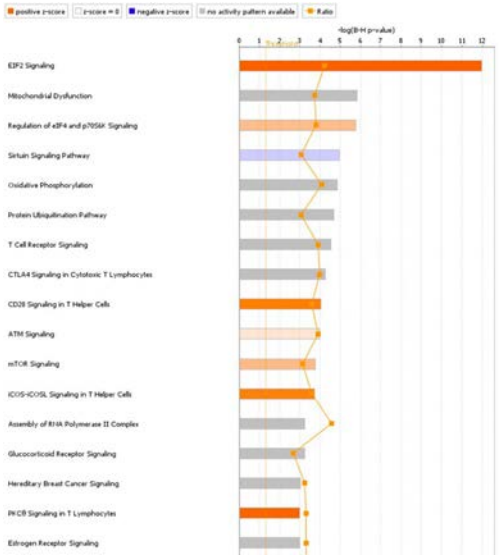

IPA to shows biologic relevance of the differentially expressed genes that were used to populate the biomarker model and confirm shared pathways between the discovery and validation cohorts.

GSEA

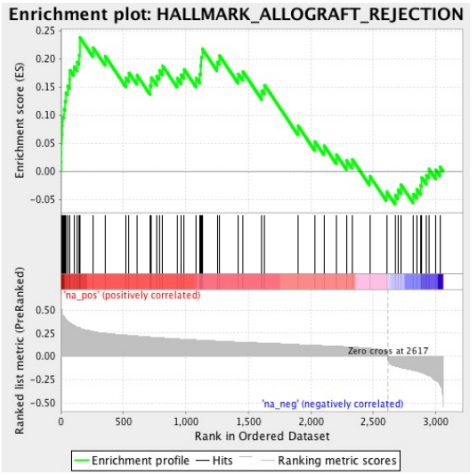

Gene Set Enrichment Analysis

Friedewald et al, Development and clinical validity of a novel blood-based molecular biomarker for subclinical acute rejection following kidney transplant, Am J Transplant . 2019 Jan;19(1):98-109

Liver Transplant + arrays + machine learning

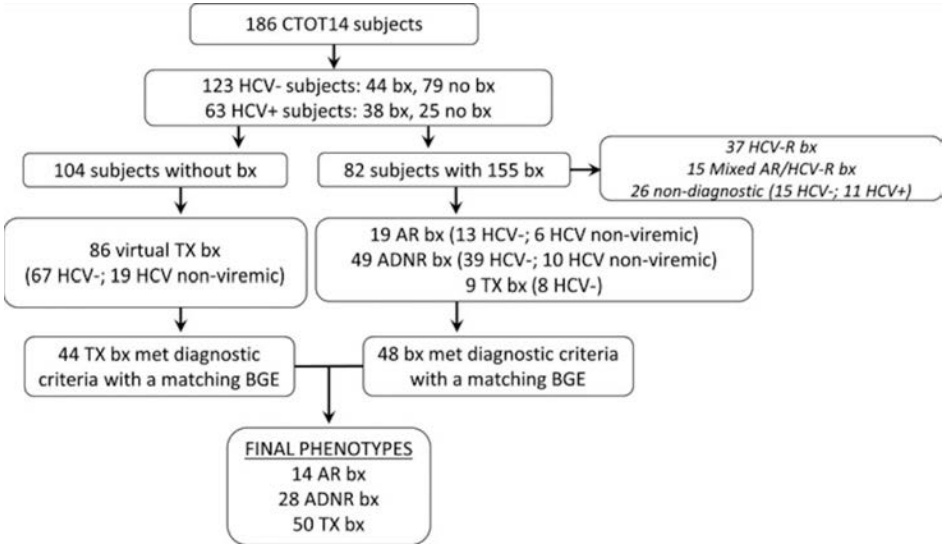

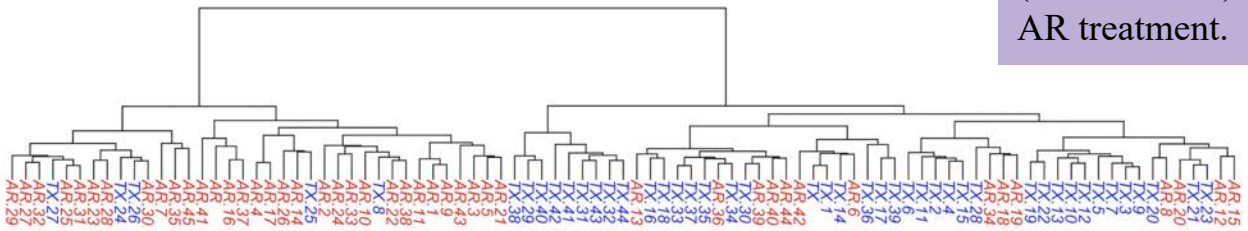

Model 1 (2019)

Normalization:	RMA
Discovery data:	NU (46 AR, 45 TX)
Algorithm :	Random forest
Features:	36 gene probe
AUC:	0.92
Validation Data:	CTOT-14 (14 AR, 50 TX)

The probability score line slopes were positive preceding AR, and negative preceding TX and non-AR (TX + ADNR) ($P \leq .001$) and following AR treatment.

Hierarchical Clustering

Levitsky et al, Discovery and validation of a novel blood-based molecular biomarker of rejection following liver transplantation, Am J Transplant . 2020 Aug;20(8):2173-2183

Liver Transplant + arrays + machine learning

2019

LME model

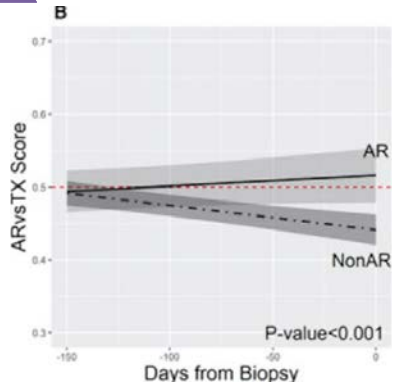

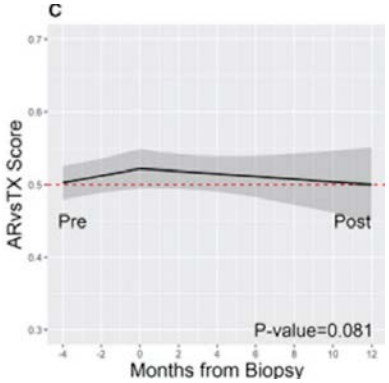

2020

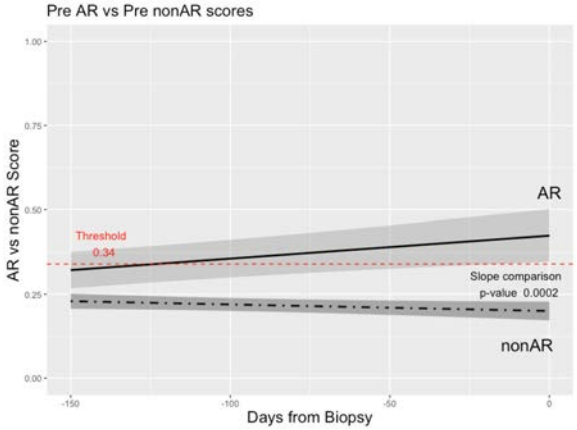

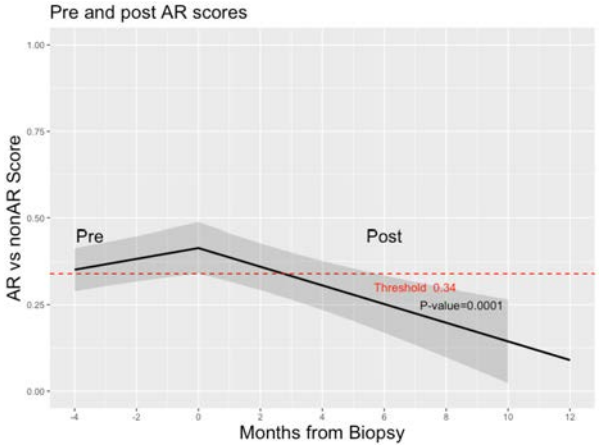

Model 2 (2020)

Normalization - fRMA
Data - 61 AR and 162 non-AR
Discovery and Validation data ratio - 70:30
Algorithm - Random forest
Features - 59 probes
AUC- 0.83

The probability score line slopes are positive preceding AR, and negative preceding nonAR (TX + ADNR) and following AR treatment

Levitsky et al, Discovery and validation of a novel blood-based molecular biomarker of rejection following liver transplantation, Am J Transplant . 2020 Aug;20(8):2173-2183

Arrays to study MCMV reactivation

Heatmap

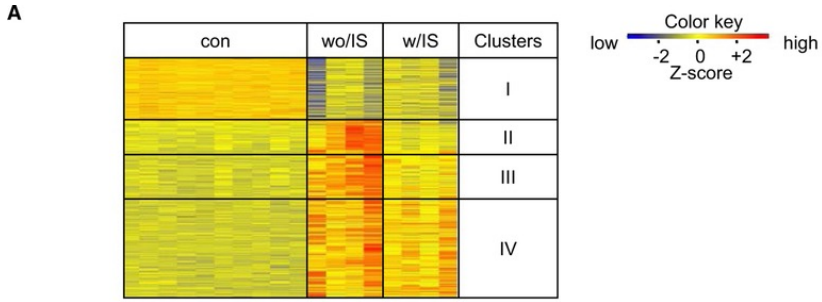

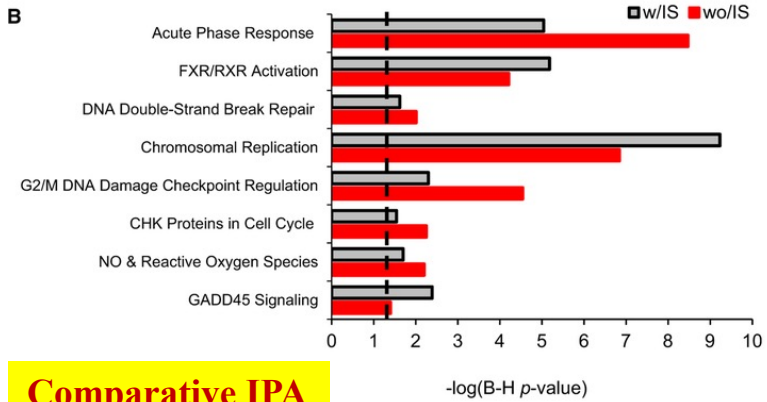

Comparative IPA

- Treatment with IS of latently infected mice alone does not induce viral reactivation, but transplant of latently infected allogeneic kidneys combined with IS facilitates MCMV reactivation in the graft and dissemination to other organs.
- The IS regimen effectively dampens allo-immune inflammatory pathways and depletes recipient anti-MCMV but does not affect ischemia-reperfusion injury pathways.
- MCMV reactivation similar to that seen in allogeneic transplants combined with also occurs after syngeneic transplants.

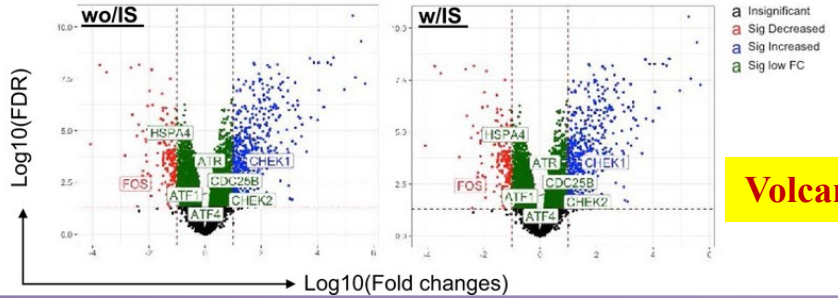

Volcano plot

Zhang Et al, A clinically relevant murine model unmasks a "two-hit" mechanism for reactivation and dissemination of cytomegalovirus after kidney transplant. Am J Transplant. 2019 Sep; 19(9): 2421-2433.

RNA-seq

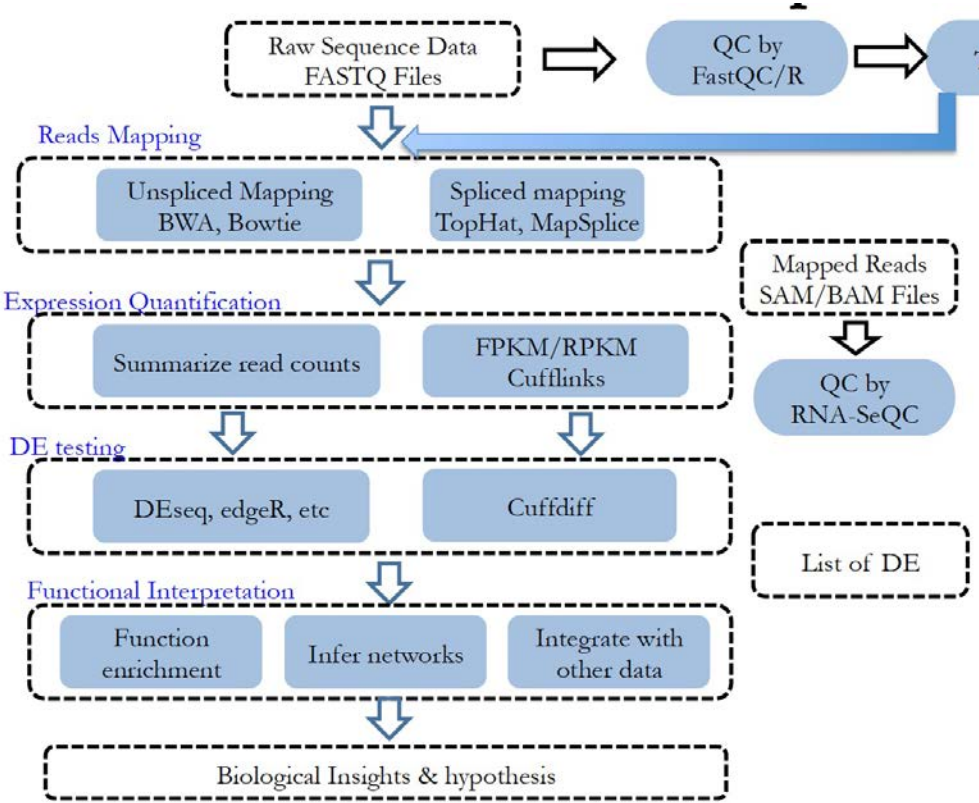

- Gene expression and differential expression
- Alternative expression analysis
- Transcript discovery and annotation
- Allele specific expression
  - Relating to SNPs or mutations
- Mutation discovery
- Fusion detection
- RNA editing

Glutamine deprivation enhances directed differentiation of renal organoids

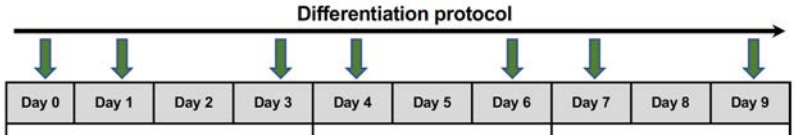

- metabolomic and transcriptomic analysis during directed differentiation reveals key pathways that play a significant role in differentiation of renal organoids, especially the alanine, aspartate and glutamate pathway

- glutamine deprivation enhances differentiation with more robust acquisition of the PAX8 marker compared to control

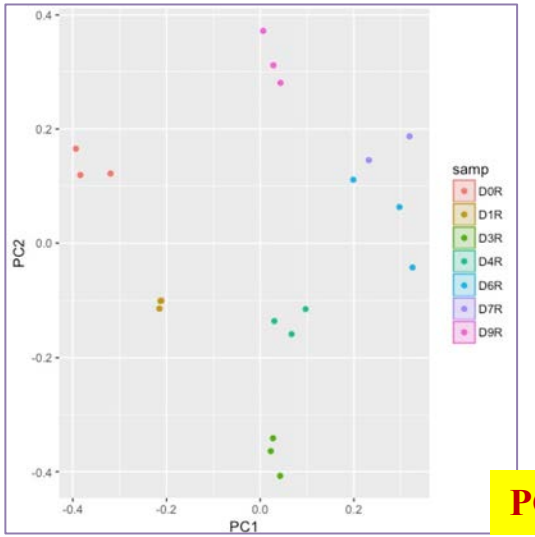

PCA

Metabolomic and RNA-seq data anlaysis

PCA

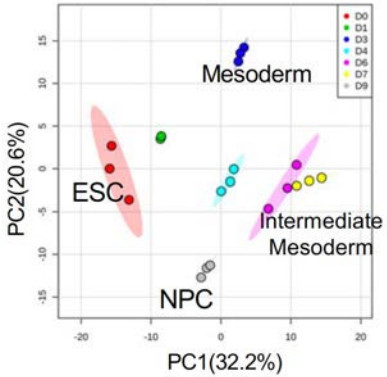

PCA analysis reveals distinct metabolic profiles from hESCs (D0) to NPCs (D9).

Venn Diagram

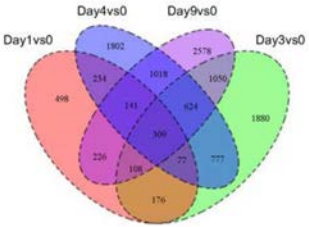

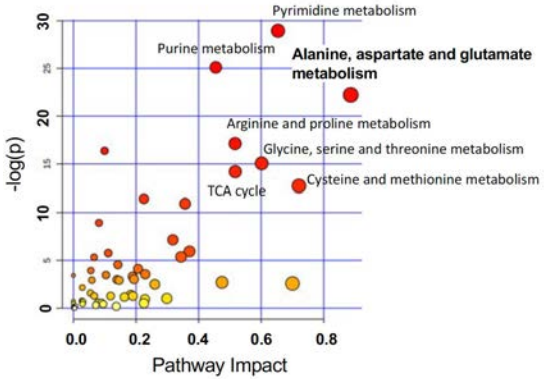

Impact analysis

Pathway impact analysis of metabolites idenitifies the alanine, aspartate and glutamate pathway as having the highest impact

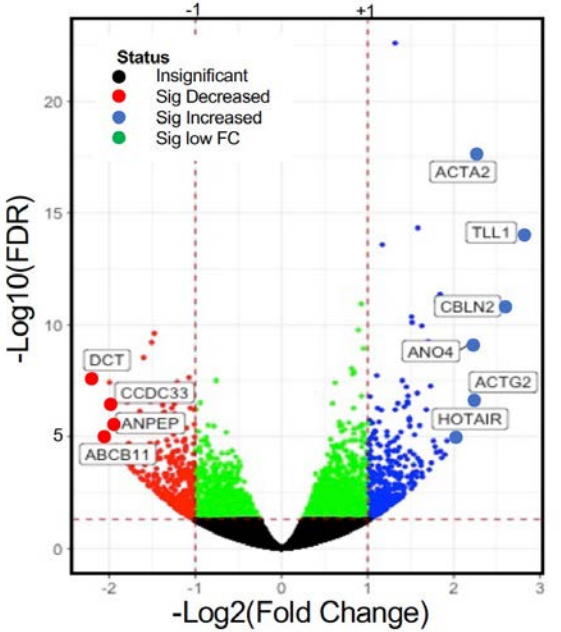

The 10 most highly expressed genes that differ between NPCs in complete media versus in glutamine deprivation conditions

Volcano Plot

ChIP-seq

ChIP-Seq identifies the binding sites of DNA-associated proteins and can be used to map global binding sites for a given protein

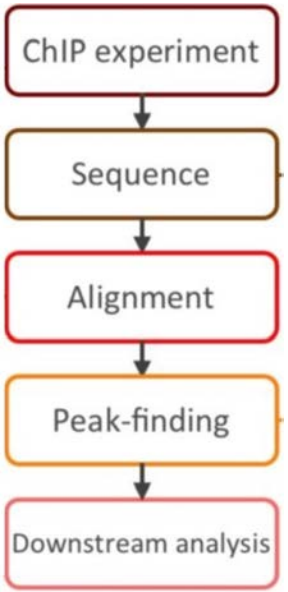

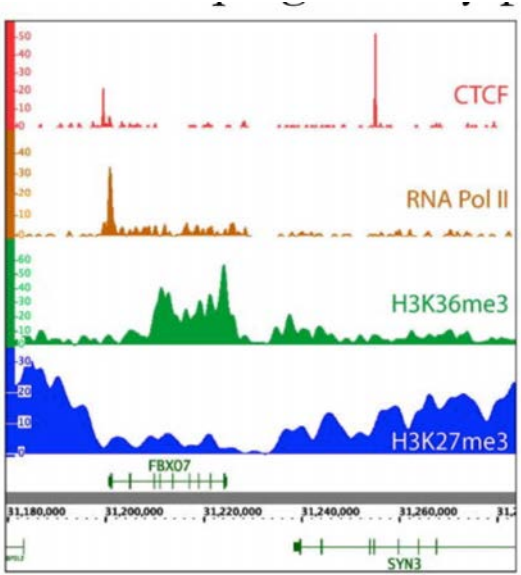

ChIP-Seq mark	Functional association
H3K4me3	Active promoters
H3K4me1	Active enhancers
H3K27ac	Active promoters and enhancers
H3K27me3	Inactive chromatin
RNA Pol II	Transcription

Modification	Transcription	Histone-modified sites
Small chemical groups		
Acetylation	Activation	H3 (K9,K14,K18,K56)
		H4 (K5,K8,K12,K16)
		H2A
		H2B (K6,K7,K16,K17)
Methylation	Activation	H3 (K4,K36,K79)
	Repression	H3 (K9,K27)
		H4 (K20)
Phosphorylation	Activation	H3 (S10)
Larger peptides		
Ubiquitylation	Activation	H2B (K 1 2 3)
	Repression	H2A (K 1 1 9)
Sumoylation	Repression	H3 (?)
		H4 (K5,K8,K12,K16)

Study of host and viral genes interactions

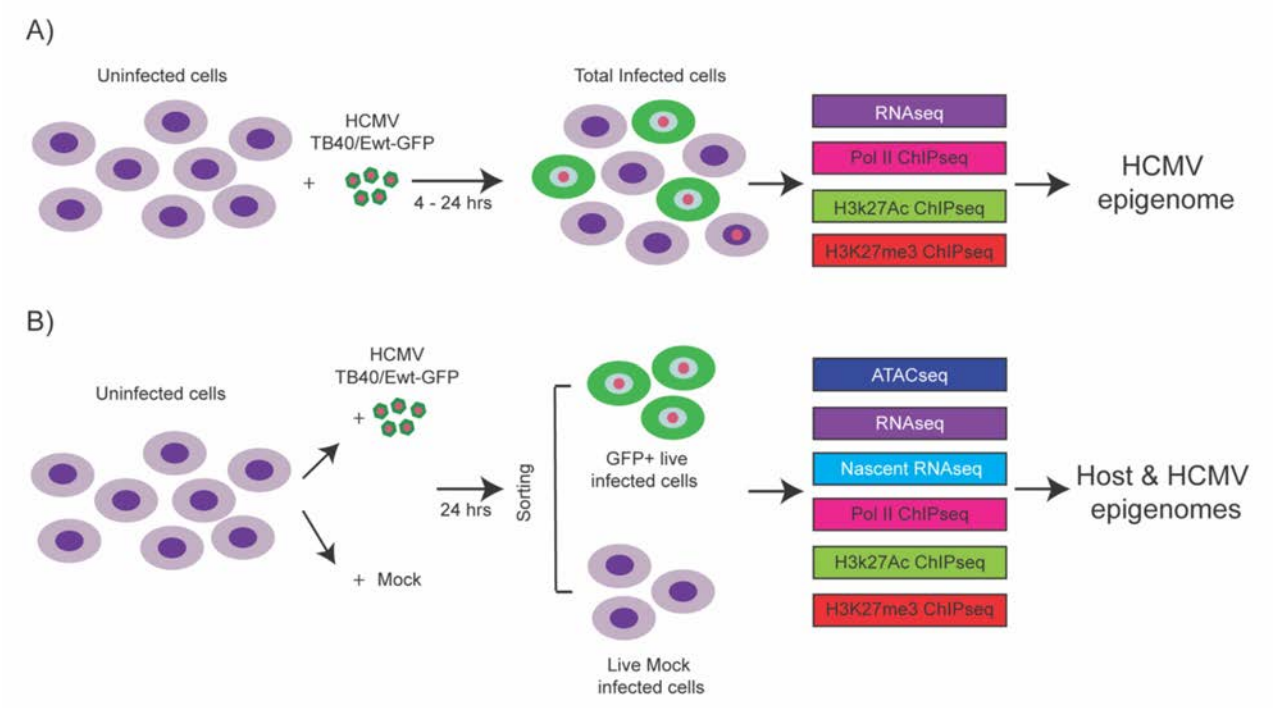

RNA-seq and ChipSeq results

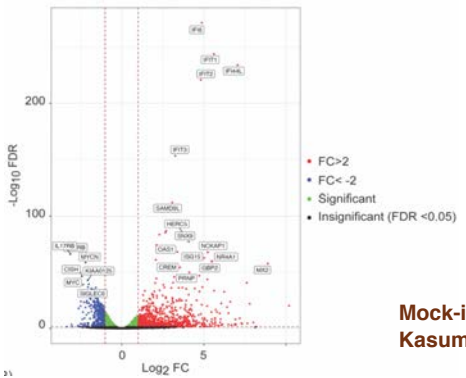

Mock-infected vs infected Kasumi-3 at 1dpi

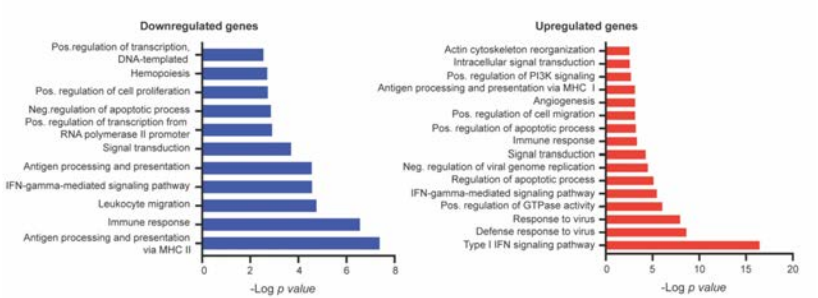

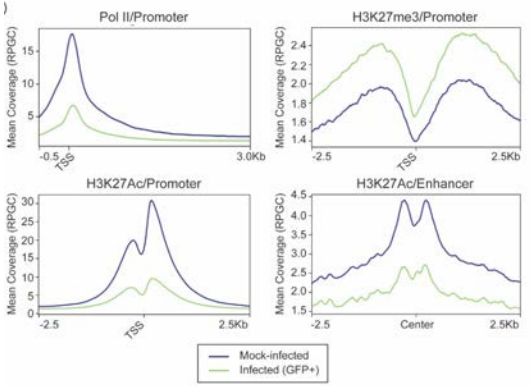

HCMV infection induces global loss of Pol II and H3K27Ac occupancy to cellular promoters

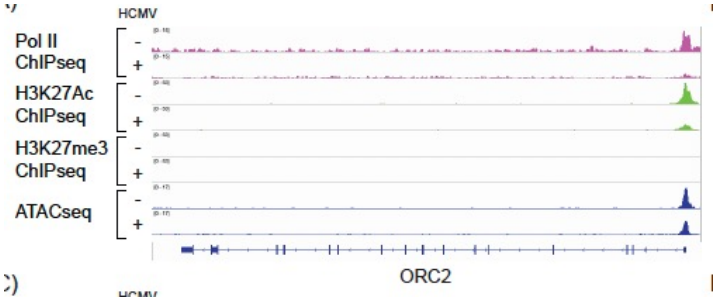

loss of de novo transcription in response to HCMV infection

Forte E. et al, Epigenetic reprogramming of host and viral genes by Human Cytomegalovirus infection in Kasumi-3 myeloid progenitor cells at early times post-infection, J Virol. 2021 Mar; https://doi.org/10.1128/JVI.00183-21

ImmunoSeq

highly optimized multiplex PCR-based assay that exclusively targets rearranged T-cell and B-cell receptor genes.

Project investigates the presence of donor reactive T cells (DRTCs) in blood and urine samples in the identification of post-transplant kidney rejection

DRTCs are identified by mixing irradiated donor PBMCs with recipient PBMCs followed by sorting for CD4 and CD8 cells and sequencing

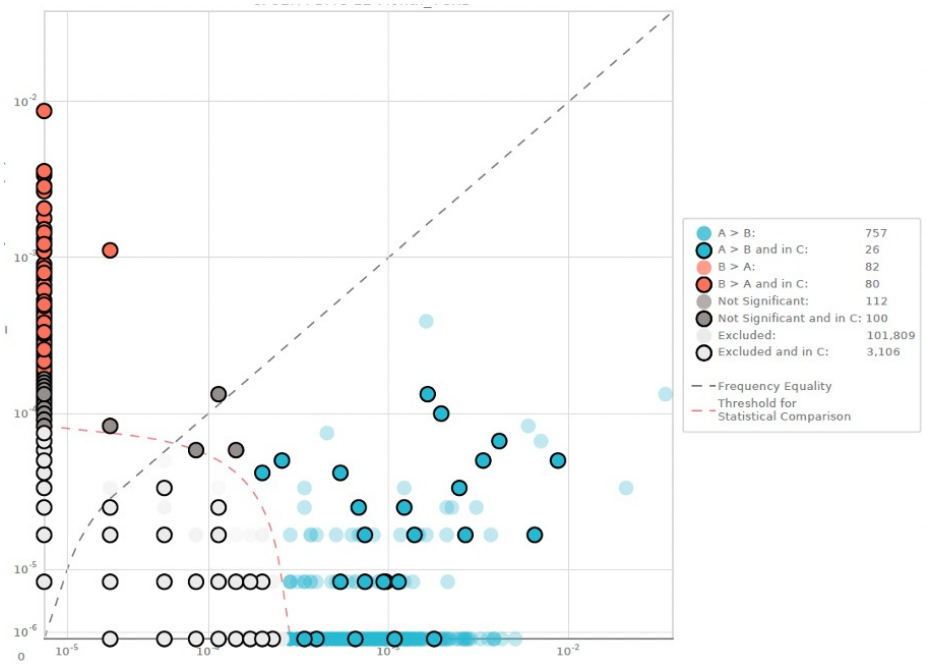

scRNA-seq

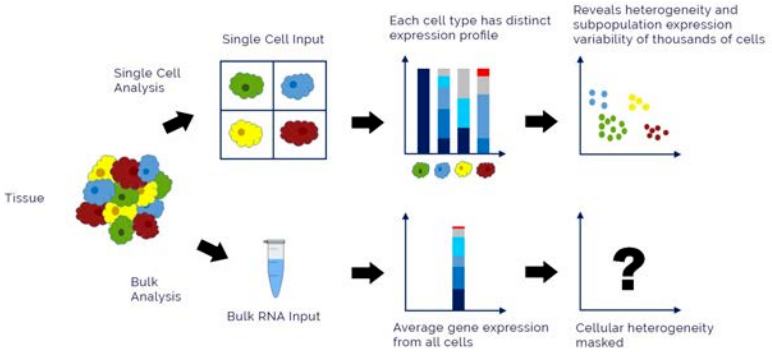

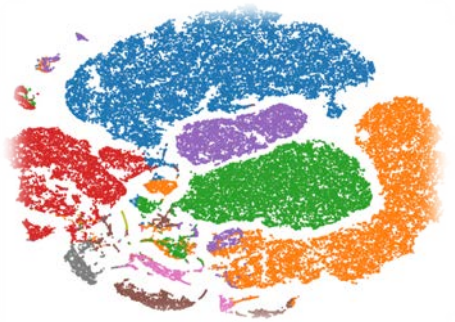

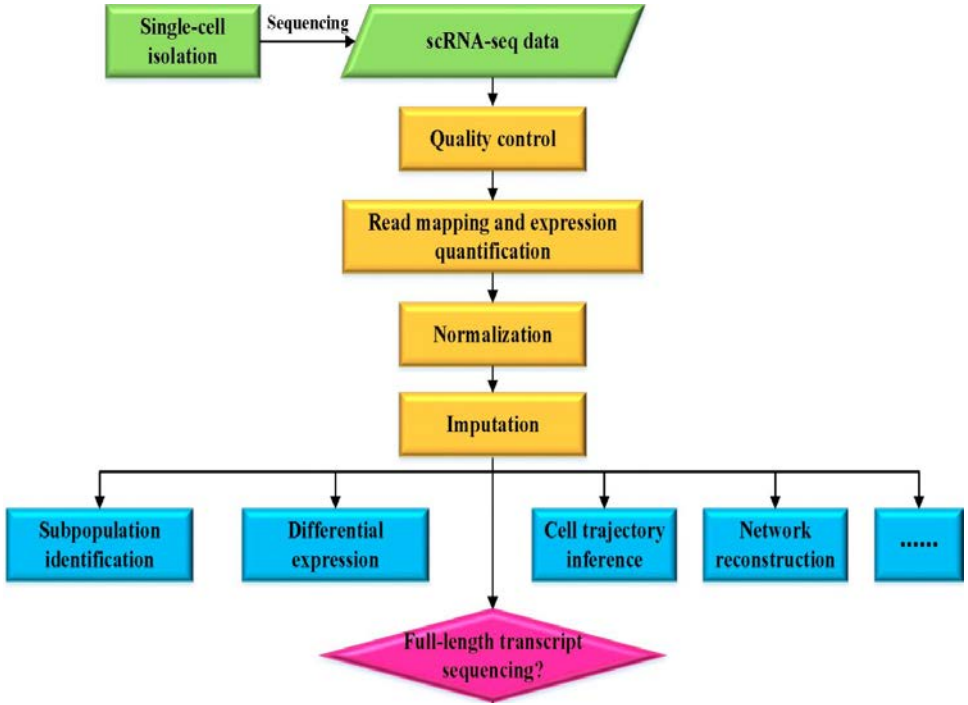

Molecular Cell doi: 10.1016/j.molcel.2017.01.023

Analyze the transcriptomics of mouse lung cells with and without latent infection of MCMV before and after transplantation

IPA CPTP vs CPTN	-log(B-H p-value)	Ratio	z-score
Th1 and Th2 Activation Pathway	11.1	0.327	#NUM!
Altered T Cell and B Cell Signaling in Rheumatoid Arthritis	10.4	0.411	#NUM!
T Helper Cell Differentiation	9.85	0.438	#NUM!
Th1 Pathway	9.39	0.347	4.218
Phospholipase C Signaling	8.96	0.256	3.571
STAT3 Pathway	8.96	0.326	0
Th2 Pathway	8.96	0.324	1.915
Role of NFAT in Regulation of the Immune Response	8.65	0.287	2.949
iCOS-iCOSL Signaling in T Helper Cells	7.3	0.324	4.382
PD-1, PD-L1 cancer immunotherapy pathway	7.3	0.33	-3.182

CD11b-CD31+

Thank You.

kandpal@northwestern.edu

Northwestern Medicine®
Feinberg School of Medicine